Sustainable Energy Technologies and Assessments 64 (2024) 103674

Contents lists available at ScienceDirect

Sustainable Energy Technologies and Assessments

journal homepage: www.elsevier.com/locate/seta

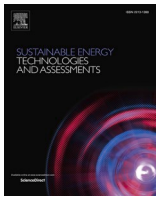

Enhancing photovoltaic module fault diagnosis: Leveraging unmanned aerial vehicles and autoencoders in machine learning

C.V. Prasshanth [a], S. Naveen Venkatesh [d], V. Sugumaran [a], Mohammadreza Aghaei [b,c,*]

[a] School of Mechanical Engineering (SMEC), Vellore Institute of Technology, Chennai, India
[b] Department of Ocean Operations and Civil Engineering, Norwegian University of Science and Technology (NTNU), 6009 Ålesund, Norway
[c] Department of Sustainable Systems Engineering (INATECH), University of Freiburg, 79110 Freiburg, Germany
[d] Division of Operation and Maintenance Engineering, Luleå University of Technology, Luleå, Sweden

ARTICLE INFO

Keywords:
Photovoltaic modules
Support vector machines
Autoencoders
Unmanned aerial vehicles

ABSTRACT

Photovoltaic (PV) modules play a pivotal role in renewable energy systems, underscoring the critical need for their fault diagnosis to ensure sustained energy production. This study introduces a novel approach that combines the power of deep neural networks and machine learning for comprehensive PV module fault diagnosis. Specifically, a fusion methodology that incorporates autoencoders (a deep neural network architecture) and support vector machines (SVM) (a machine learning algorithm) is proposed in the present study. To generate high-quality image datasets for training, unmanned aerial vehicles (UAVs) equipped with RGB cameras were employed to capture detailed images of PV modules. Burn marks, snail trails, discoloration, delamination, glass breakage and good panel were the conditions considered in the study. The experimental results demonstrate remarkable accuracy of 98.57% in diagnosing faults, marking a significant advancement in enhancing the reliability and performance of PV modules. This research contributes to the sustainability and efficiency of renewable energy systems, underlining its importance in the quest for a cleaner, greener future.

Introduction

A solar cell, also referred to as a photovoltaic (PV) cell, acts as the cornerstone in converting solar energy into electricity through the photovoltaic effect. This PV cell forms the basic unit within a PV generator which in turn serves as the central component of a solar generator system. The PV generator comprises an array of interconnected PV modules, allowing for versatile configurations such as series, parallel or combinations of both catering to specific energy needs and environmental conditions [1]. These photovoltaic modules represent organized assemblies of interconnected PV cells, efficiently capturing sunlight and converting it into electrical energy while streamlining system installation and maintenance. PV technology boasts versatile applications like solar farms supply utility-scale power to grids while remote areas benefit from off-grid PV, serving rural homes, offshore platforms and clinics. In urban and remote locales, PV powers stand-alone devices, from emergency phones to road lighting [2]. Its reach extends beyond Earth, fuelling space missions. For terrestrial use, PV integrates into buildings, providing renewable energy, and serves military and transportation needs with lightweight, flexible solutions, exemplifying its adaptability and versatility. Currently, renewable energy sources contribute 6% of the total electricity production, with the potential to increase significantly to 38% by 2040. Among the various renewable energy options, solar energy has emerged as a pivotal player in the realm of electricity generation [3].

PV modules are susceptible to a range of issues including burn marks, snail trail, discoloration, delamination and glass breakage, all of which can significantly impact their performance and longevity [4]. Recent findings indicate that these faults collectively lead to an annual power output loss of 18.9% for PV modules [5]. Therefore, implementing proactive measures for identifying and diagnosing these faults is crucial to ensure the optimal functioning and extended lifespan of solar energy systems. However, the emergence of artificial intelligence (AI) heralds a transformative breakthrough. AI, particularly in the field of computer vision, boasts widespread applications in computer-aided inspection, industrial control systems and robotic navigation. Notably, AI can be instrumental in monitoring machinery and mechanical components for faults through automated image analysis. With the integration of machine learning and deep learning, AI makes it not only feasible, however it also makes it significantly more precise to diagnose machinery faults from images [6]. This innovative approach holds the potential to

* Corresponding author.
E-mail address: mohammadreza.aghaei@ntnu.no (M. Aghaei).

https://doi.org/10.1016/j.seta.2024.103674
Received 4 October 2023; Received in revised form 6 February 2024; Accepted 11 February 2024
Available online 17 February 2024

Nomenclature

PV	Photovoltaic
SVM	Support Vector Machines
UAVs	Unmanned Aerial Vehicles
RGB	Red, Green, Blue
IBK	K-nearest neighbor
PVMs	Photovoltaic Modules
CNNs	Convolutional Neural Networks
AI	Artificial Intelligence
GANs	Generative Adversarial Networks
AM	Air Mass
UV	Ultraviolet
EVA	Ethylene Vinyl Acetate
MSE	Mean Squared Error
RBF	Radial Basis Function
RMSE	Root Mean Squared Error
MAE	Mean Absolute Error

revolutionize the maintenance and optimization of PV modules, enhancing their lifespan and reliability by providing advanced early detection and fault diagnosis capabilities that surpass conventional methods.

Extensive research has been carried out in the field of fault diagnosis for PV modules. For instance, Kellil et al., proposed the application of a fine-tuned VGG-16 Convolutional Neural Network for fault diagnosis of PV modules using thermographic images, offering a technique to address the stability, reliability, and security challenges associated with decentralized photovoltaic systems [7]. Jerome Vasanth et al., introduced an innovative approach for fault detection in PV modules, leveraging deep learning and machine learning techniques applied to RGB images. Their study demonstrated the effectiveness of feature extraction using various pretrained networks and identified DenseNet-201 combined with k-nearest neighbor (IBK) classifier as the best-performing combination, achieving a remarkable classification accuracy [8]. Sridharan et al., presented an innovative approach for diagnosing visual faults in photovoltaic modules (PVMs) using convolutional neural networks (CNNs) to extract distinct image patterns associated with common PV module faults, followed by feature selection with the J48 decision tree algorithm. Their study explored various decision tree-based classifiers, with the random forest algorithm emerging as a potential model for real-time fault diagnosis [9]. Tsanakas et al., introduced an alternative approach for diagnosing faults in PV modules, utilizing thermal image processing and the Canny edge detection operator to identify hot-spot formations in defective cells. Their study demonstrated promising results in detecting performance-affecting issues, complementing conventional electrical monitoring methods for enhanced fault detection in PV modules [10]. Hu et al., presented a parameter-based model for fault diagnosis of PV modules, which incorporates electrical modeling and an energy balance equation. This model utilizes key parameters derived from real-world data, such as total effective solar energy, heat exchange coefficients, and ambient temperature, obtained from thermal imaging, offering a valuable approach for PV module fault diagnosis [11]. These findings highlight the significance of integrating AI-driven fault diagnosis methodologies for timely detection and mitigation of issues in PV module, enhancing their reliability and performance.

In recent times, the utilization of unmanned aerial vehicles (UAVs) has emerged as a promising solution for inspecting faults in PV modules. These UAVs have witnessed significant technological advancements, particularly through their integration with thermal cameras [12]. However, this system has certain limitations, particularly when it comes to detecting hotspots at higher temperatures. Hotspots serve as crucial indicators of potential issues such as partial shading, microcracks, solder bond failure, corrosion and short circuits [13]. Since, thermal images are represented as pseudo-colour images based on thermal radiation data, identifying these specific fault occurrences can be challenging. In the present study, in order to address these limitations, there has been a transition towards replacing thermal-imaging cameras with high-resolution digital cameras mounted on UAVs. These high-resolution cameras capture true-color images from photovoltaic modules, facilitating the identification of visible defects like burn marks, snail trail, discoloration, delamination and glass breakage with remarkable precision. This transition not only enhances the overall fault detection capabilities of UAVs; however, it also ensures that even minor faults can be spotted accurately. This evolution in inspection technology represents a significant step forward in the maintenance and optimization of PV modules, offering a comprehensive and efficient solution for fault detection and diagnosis.

Autoencoders are neural network architectures used for learning that aim to encode and decode input data, preserving essential information in an intermediate representation. This makes autoencoders valuable tools for feature extraction and data compression in various applications [14]. The integration of autoencoders with machine learning for image classification proves to be a compelling approach. Autoencoders effectively learn and extract pertinent features from raw image data, reducing dimensionality, denoising images and facilitates transfer learning, thereby saving valuable resources. These fusion harnesses the nonlinear capabilities of machine learning models to capture intricate data relationships while serving as an effective technique [15]. This combined framework presents a promising avenue for enhancing image classification performance, a key focus of our research.

In fault detection in PV modules, several limitations impede progress. Notably, the predominant focus on thermal or electroluminescence images has left true color or RGB images largely unexplored for diagnosing faults in PV modules, creating a gap in research direction. Compounding this issue is the limited availability of diverse image data in public repositories, hindering the development and validation of fault detection methodologies. Despite the proven efficiency of UAVs in reducing monitoring time and manpower, the absence of a publicly available and comprehensive PV module fault dataset poses a significant challenge. The exploration of fault detection methods has seen promising strides in individual applications of machine learning and deep learning; however, the combined approach of these techniques is still in its early stages. Within these limitations, there is an opportunity for innovation. Integrating true color or RGB images into fault diagnosis methodologies, coupled with the continued use of UAVs, holds promise for enhancing the accuracy of fault detection in PV modules. To address computational demands, alternatives to Generative Adversarial Networks (GANs) are suggested for data enhancement, including basic image transforms like noise, shift, warp, flip, rotation, zoom, and blur performed without GAN usage. Additionally, the unexplored combination of autoencoders with Support Vector Machines (SVM) introduces a novel dimension to the research landscape, offering a unique and effective solution to advance the field of PV module fault detection. This integrated approach leveraging machine and deep learning techniques, along with novel methodologies like autoencoders with SVM, presents a path towards more robust fault detection in PV modules, addressing the current research gaps and fostering innovation in the field.

The paper is structured into distinct sections to systematically present the experimental studies and analysis. In Section 2, the experimental studies are detailed, starting with the Experimental Setup and then delving into the visual faults observed in PV modules, such as Burn Marks, Snail Trail, Discoloration, Delamination and Glass Breakage. Following this, Section 3 outlines the methodology employed in the study, encompassing Data Augmentation, Feature Extraction utilizing Autoencoders and Feature Classification using Support Vector Machines. Section 4 focuses on presenting and discussing the results obtained from the study. It covers the impact of varying C values, gamma

and kernel types on SVM performance, concluding with a comparative analysis against other cutting-edge works in the field. Section 5 summarizes the main findings and draws overall conclusions based on the studys results and suggests direction for future research.

Experimental studies

This section offers an overview of the experimental arrangement and process, delineating the complete methodology used in the research.

Experimental setup

A surveillance system utilizing an UAV equipped with a high-quality professional camera, various on-board processors, a ground control centre and sensors comprises the experimental setup. In laboratory conditions, aerial photographs of photovoltaic modules (PVM) were captured using a DJI Mavic 2 Zoom drone fitted with an RGB professional camera which was operated remotely via a handheld controller. These captured photos were wirelessly transmitted to the ground control station and then stored in a designated storage container using data cables or memory cards. Subsequently, the acquired images underwent offline processing, employing autoencoders and machine learning techniques, along with an analysis of classification results. Fig. 1 illustrates the PV module platform.

To gather images, the modules were strategically placed at six different locations within the facility. The data collection involved the examination of five flawed modules and one flawless module for UAV image acquisition. The drone was directed to fly at altitudes ranging from 1 to 5 m above the PVM during data collection. Each PVM test condition, such as burn marks, snail trail, discoloration, delamination, glass breakage and good panels, was set up at various locations across the facility. During each session, which lasted approximately 14 min, a total of 100 photos were captured for each specific condition. Supplementary Fig. 2, provides a sample of the acquired images. All measurements were conducted under standard test conditions, including a temperature of 25°C, irradiance of 1000 W/m^2 and Air Mass (AM)1.5. AM1.5 is a standardized sunlight spectrum used for testing solar cells and panels under controlled conditions.

Visual faults in PV module

PVM systems are susceptible to faults triggered by fluctuating climatic conditions, environmental uncertainties, and thermal stress. These vulnerabilities can lead to system instability and reduced energy production, impacting overall performance and reliability. Supplementary Fig. 3, represents the various fault images.

Burn marks

Burn marks in PV modules, often arises from failed solder bonds, ribbon tears in PV cells, or localized heating events that can pose a dual concern of safety and performance. These marks can lead to electrical malfunctions and safety hazards within the PV system while also disrupting the modules electrical flow, resulting in decreased performance and reduced power output. To ensure the safety and optimal functioning of PV modules, it is imperative to promptly detect and address burn marks through regular maintenance and quality control measures [16].

Snail trail

Snail trails in PV modules are indicative of microcracks originating from cell corners that aggravates due to thermal stress, UV radiation and high temperatures with accelerated formation in summer due to increased thermal stress. Material selection for back covers and lamination layers also plays a role in snail trail development alongside microcracks, UV exposure, mechanical load and freezing. The appearance of pale grey or black coloration in silver interconnects signals the presence of snail trails. Once evident, these trails are irreversible, necessitating panel replacement and causing quicker module degradation [17].

Discoloration

Discoloration in PV modules, characterized by a brown or yellow tint, results from UV and thermal stress. It alters light transmittance, reducing sunlight absorption and causing power loss. Discoloration occurs due to chemical reactions within the encapsulant material when exposed to water and UV rays at high temperatures. The fault is driven by increased heat, humidity and UV radiation exposure leading to power loss and noticeable colour changes in PV modules, like yellowing or browning [18].

Delamination

Delamination in PV modules arises from a loss of adhesive properties between PV cells and ethylene vinyl acetate (EVA) encapsulants, particularly in changing climates. This issue mainly occurs at corners and edges of PV modules, leading to water penetration, reduced radiation absorption, increased reflection, electrical problems and power loss. Delamination is driven by the weakening bond between glass, encapsulant and the rear cover exacerbated by exposure to moisture and heat which can elevate salinity levels. Ultimately, it results in corrosion from

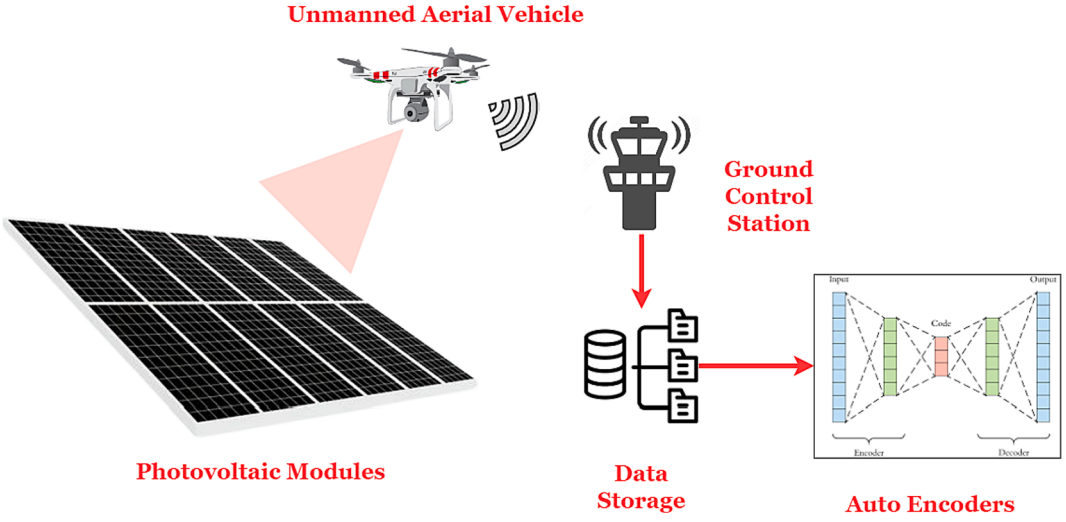

Fig. 1. PV module platform.

moisture intrusion, impacting the long-term performance and efficiency of PV modules [19].

Glass breakage

Glass breakage in PV modules can stem from various sources including, harsh weather conditions, improper installation, transportation shocks and thermal stresses. Although the tempered glass used in PV modules can initially withstand breakage without impairing functionality, it permits moisture infiltration leading to oxide formation and interconnect corrosion, ultimately diminishing the modules long-term performance and efficiency. Additionally, PV modules are susceptible to physical damage during installation and transit, as well as thermal stresses, which collectively result in reduced radiance, corrosion, and moisture infiltration, affecting their long-term efficiency [20].

Methodology

In this research study, the integration of autoencoders and support vector machines (SVM) has been demonstrated to offer a compelling synergy between deep learning and traditional machine learning. The investigation focuses on utilizing an UAV to gather image data from diverse PV module test scenarios. Starting with an initial dataset of 600 images, data augmentation techniques were employed to create a balanced and robust dataset containing 3,150 images, with 525 images representing each PV module scenario. These augmentation techniques encompassed various transformations such as blurring, flipping, rotating, adding noise, shifting, zooming, and warping, which effectively diversified the dataset while preserving its authenticity. The pivotal role of autoencoders came into play as they were employed to extract essential features from this augmented image dataset with the aim of capturing pertinent information from PV module images. These extracted features were subsequently utilized for the classification of different PV module conditions using the formidable SVM algorithm, renowned for its proficiency in handling high-dimensional data. Supplementary Fig. 4, provides a comprehensive illustration of the process involved in fault classification in PV module.

Furthermore, the study delved into the analysis of confusion matrices to assess the classifiers ability to effectively differentiate between various PV module conditions. The outcomes obtained from this comprehensive evaluation were meticulously scrutinized and interpreted, providing valuable insights into the efficacy of the proposed approach in accurately classifying PV module conditions based on image data. This research underscores the potential of combining deep learning feature extraction capabilities with the robust classification prowess of SVM to enhance the field of image-based PV module condition monitoring and assessment.

Data augmentation

Data augmentation is a pivotal technique in modern machine learning, particularly in domains like computer vision where obtaining large volumes of high-quality annotated data is often a challenge. It serves as a vital solution to address data scarcity and the manual efforts required for data collection and annotation. Data augmentation involves creating new training data by applying various transformations to existing dataset such as blurring, flipping, rotating, adding noise, shifting, zooming and warping. This not only increases data volume; however, it also enhances data quality and diversity making models more robust to real-world conditions. In essence, data augmentation plays a critical role in improving model generalization and performance, making it an indispensable component in the machine learning toolbox for addressing data-related challenges [21].

Feature extraction using autoencoders

Autoencoders are neural network-based models designed to capture essential data patterns and represent them in a reduced dimension. The process can be performed by transforming input data into a lower-dimensional encoding using a bottleneck layer to define the encodings dimension and then reconstruct the original data from this encoding through a decoder [22]. Supplementary Fig. 5, displays the neural networks encoder and decoder components. Specifically, Phi corresponds to the encoding parameters of the encoder, while Theta pertains to the decoding parameters of the decoder. A fundamental autoencoder comprises of three primary components that work in tandem to perform a crucial task in unsupervised learning. First, the encoder, which plays a pivotal role in the network takes the input data and skilfully compresses it into a lower-dimensional encoding (significantly reducing its dimensionality). The number of nodes in this layer determines the dimension of the encoding and influences the quality of the learned representations. Next, the bottleneck layer carries out the encoding operation that is designed with fewer nodes than the input layer wherein the dimensionality of the data is further reduced. Remarkably, it retains essential information, capturing the underlying patterns and structures within the input data. Lastly, the decoder takes the encoding produced by the bottleneck layer and endeavour to reconstruct the original data from it.

Through learning and adaptation, the decoder becomes proficient at capturing and reproducing the critical patterns in the data, allowing for precise data reconstruction. The encoding produced by the bottleneck layer serves as a condensed representation of the data, revealing intricate relationships within the dataset [23]. Decoders, on the other hand, work in tandem with encoders to reconstruct the input from the compressed latent space. The symmetric structure ensures a faithful reproduction of the original input by mirroring the encoding layers. Supplementary Fig. 6, represents an example of an auto encoded image of a PV module.

During training, autoencoders typically minimize a loss function such as mean square error or binary cross entropy. This loss function quantifies the error between the input data and the reconstructed output, guiding the model to adjust its weights and biases to minimize this error and improve its ability to capture and reproduce data patterns. In the present study, the autoencoder architecture for image reconstruction adopts an input layer tailored to 32x32 RGB images, followed by encoding layers with a flexible number of layers (3 to 10) employing ReLU activation. Symmetric decoding layers mirror the encoding structure, utilizing ReLU activation. The output layer, a Dense layer with Sigmoid activation, reconstructs the input. Training parameters involve the Adam optimizer, Mean Squared Error loss, with a batch size of 32 using both training and validation data. The specified training parameters constitute a well-thought-out configuration for training an autoencoder with a focus on feature extraction. The utilization of the Adam optimizer brings the advantages of adaptive learning rates, efficient handling of sparse gradients, and robustness to hyperparameter choices. MSE loss is aptly chosen for the objective of minimizing the disparity between predicted and true values. A batch size of 32 introduces beneficial noise during training, aiding generalization, while the separation of training and validation data ensures an accurate assessment of the models performance on unseen examples, preventing overfitting. Feature extraction in the encoding layers signifies a latent space representation, emphasizing the capture of essential input features. The tuning process, involving the exploration of layer configurations and units per layer, is guided by the objective of minimizing validation loss, thereby striking a balance between model complexity and generalization. Table 1 represents an overall summary of the autoencoders model by layers.

Feature classification using SVM

A SVM is a supervised machine learning algorithm used for classification tasks. It takes a labelled dataset with feature vectors as input. SVM operates in a high-dimensional feature space, aiming to find an optimal hyperplane that separates the data into different classes as

Table 1
Model summary by layers.

Layer name	Layer type	Activation Function	Number of units	Number of Parameters	Output shape
Input layer	Input	–	–	0	[(None, 32, 32, 3)]
Encoder_dense_1	Dense	ReLU	256	1024	(None, 32, 32, 256)
Encoder_dense_2	Dense	ReLU	256	65,792	(None, 32, 32, 256)
Encoder_dense_3	Dense	ReLU	256	65,792	(None, 32, 32, 256)
Decoder_dense_1	Dense	ReLU	256	65,792	(None, 32, 32, 256)
Decoder_dense_2	Dense	ReLU	256	65,792	(None, 32, 32, 256)
Decoder_dense_3	Dense	ReLU	256	65,792	(None, 32, 32, 256)
Output layer	Dense	Sigmoid	3	771	(None, 32, 32, 3)
Total parameters:				330,755	

represented in Supplementary Fig. 7. The key focus is on constructing a hyperplane that maximizes the margin, or spatial gap, between bounding planes on either side of the primary separating plane. This emphasis on achieving maximum separation contributes to SVMs effectiveness in minimizing errors during the classification of unknown data points.

This hyperplane maximizes the margin between the closest data points of each class, known as support vectors [24]. SVMs can handle non-linear data using kernel functions that implicitly map the data into a higher-dimensional space where it becomes linearly separable. The decision function of an SVM computes a decision value for each data point, and the sign of this value determines the predicted class label. A regularization parameter (C) balances margin maximization and classification error minimization. SVM algorithms utilizes a collection of mathematical functions known as kernels, including the linear, poly, sigmoid and RBF as represented in Table 2. During training, SVM employs optimization algorithms to find the optimal hyperplane efficiently. Hyperparameter tuning is vital in SVMs, involving parameters like 'C' (which balances margin and classification error), the choice of kernel function (e.g., linear, RBF), and kernel-specific parameters (e.g., 'gamma' for RBF). Tuning these hyperparameters, often done via techniques like grid search or cross-validation, is crucial to achieving the best model performance for specific datasets and classification problems [25].

Results and discussions

In the process of analyzing RGB images of the PV modules captured from UAVs, the critical stages entail feature extraction using autoencoders and subsequent classification employing SVMs. Autoencoders play a pivotal role in dimensionality reduction while preserving crucial information within the images. Once features are extracted through the encoding process, a crucial step involves tuning the autoencoder architecture. This tuning process often includes varying the number of layers and units to optimize the models ability to capture and represent the underlying patterns in the data. The goal is to find a configuration that strikes the right balance between compression and information preservation. After the autoencoder is appropriately tuned, the extracted features are then fed into an SVM model, where the choice of hyperparameters, including C, gamma, and kernel type, is pivotal for optimizing classification accuracy. The dataset is divided into training (80%) and testing (20%) subsets to facilitate an unbiased evaluation of the trained SVM models performance. In this section the effect of varying the hyperparameters manually is discussed. Manual hyperparameter tuning remains essential despite automated methods. It leverages domain expertise and intuition, aligning parameter choices with specific data characteristics. Manual tuning provides transparency, aiding understanding of each hyperparameters impact for troubleshooting and refinement. While automated methods offer efficiency, manual tuning is preferred for a nuanced, context-aware approach in a well-defined search space. Its human-driven, iterative nature ensures a tailored exploration of configurations, aligning the model closely with practitioner insights and data nuances.

Table 2
Kernel function and its mathematical formulas.

Kernel Function	Formula
Linear	$K(x_i, x_j) = x_i^T x_j$
Polynomial	$K(x_i, x_j) = (x_i^T x_j + c)^d$
Radial Basis Function	$K(x_i, x_j) = e^{\left(-\frac{\|x_i - x_j\|^2}{2\sigma^2}\right)}$
Sigmoid	$K(x_i, x_j) = \tanh(\propto x_i^T . x_j + c)$

In the present study, our approach involves a two-step process where we first employ autoencoders followed by SVM classification. For the evaluation of the autoencoders performance in learning fault-free representations, we utilize the validation loss as a crucial metric. The validation loss signifies how well the autoencoder can reconstruct PV module data without faults, providing insight into its ability to capture normal patterns. Subsequently, during the SVM classification stage, our assessment incorporates key classification metrics, including accuracy, F1 score, precision, and recall. These metrics collectively offer a comprehensive evaluation of the SVM models proficiency in accurately classifying faults within the photovoltaic modules. The F1 score, striking a balance between precision and recall, proves particularly valuable in scenarios where achieving a harmonized performance in both aspects is essential for robust fault detection. By employing this dual-phase evaluation strategy, we ensure a thorough examination of the fault diagnosis capabilities of our integrated system, demonstrating its potential for enhancing the maintenance and performance monitoring of photovoltaic systems.

Effect of number of layers and units in autoencoders

In autoencoders, the architecture is defined by layers, representing the hierarchical levels of the neural network, and units, indicating individual processing nodes within each layer. The interaction between the number of layers and units plays a crucial role in shaping the models ability to capture and reconstruct features during the dimensionality reduction process. Increasing the number of units allows for a more detailed encoding of features, potentially capturing finer details in the data, but at the cost of higher computational demands. Conversely, reducing the number of units may simplify representations, introducing the risk of information loss but offering the advantage of decreased computational complexity. Striking a balance in the configuration of both layers and units is essential, as it determines the autoencoders effectiveness in capturing and retaining essential features within the input data finding the delicate equilibrium between representation intricacy and computational efficiency. Table 3 presents the effect of varying the number of layers and units. The combination of three layers with 256 units each demonstrates superior performance, showcasing a relatively lower validation loss compared to other configurations. This particular autoencoder setup is employed as the method for feature extraction in subsequent analyses.

Table 3
Effect of varying the number of layers and units.

Validation Loss				
Number of layers	Number of units			
	32	64	128	256
3	0.006351	0.002357	0.001021	0.000575
4	0.003318	0.001724	0.001214	0.001031
5	0.004061	0.001959	0.001164	0.00098
6	0.002364	0.001334	0.001249	0.001522
7	0.016716	0.001921	0.001606	0.001483
8	0.045638	0.00205	0.001515	0.001911
9	0.004344	0.001842	0.001996	0.002251
10	0.035464	0.002374	0.002402	0.002839

Effect of C value in SVMs performance

In SVMs, the "C" parameter is a critical hyperparameter that controls the balance between maximizing the margin and minimizing the classification error. With the increase in the value of C, the SVM becomes less tolerant of misclassified data points. This means it strives to classify all training points correctly, even if it means sacrificing the margin, the distance between the decision boundary and the nearest data points (support vectors). Conversely, decreasing the value of C makes the SVM more tolerant of misclassified data points, allowing for a larger margin between classes. This larger margin reflects a greater emphasis on generalization to unseen data rather than fitting the training data perfectly. Smaller C values encourage a simpler decision boundary that tends to generalize better. Table 4 illustrates the influence of adjusting the C value. Notably, the highest accuracy of 97.30% is achieved with a C value of 10, this C value will be fixed while the remaining hyperparameters are varied to find the best combination.

Effect of gamma in SVMs performance

In SVMs, the hyperparameter 'gamma' holds pivotal importance in shaping the models behaviour, especially when employing the Radial Basis Function (RBF) kernel. It dictates the flexibility and complexity of the decision boundary, making its selection crucial for optimal model performance. To streamline 'gamma' choice, Scikit-Learn offers 'scale' and 'auto' heuristic options. 'Scale' automatically calculates 'gamma' as 1 / (n_features * X.var()), adapting it to feature scales, which is beneficial for datasets with varying feature magnitudes. Conversely, 'auto' sets 'gamma' to 1/n_features, ensuring a consistent 'gamma' value regardless of dimensionality, simplifying SVM setup, and making it suitable for situations with unknown data characteristics or high-dimensional datasets. These automatic 'gamma' choices facilitate SVM implementation, enhancing accessibility and efficiency in model selection. Table 5 illustrates the impact of different gamma values while keeping the previously determined optimal C value constant. In this experiment, gamma is adjusted, and the results demonstrate that the 'scale' setting outperforms the 'auto' setting.

Effect of kernel in SVMs performance

Kernels are mathematical functions used to transform input data into higher-dimensional spaces, facilitating the discovery of linear decision boundaries, even when the original data isn't linearly separable. The key objective of SVM is to maximize the margin between two classes of data points. Kernels, such as the Linear Kernel for linearly separable data, the Polynomial Kernel introducing non-linearity with a degree parameter, the RBF Kernel using Gaussian functions with a gamma parameter and the Sigmoid Kernel uses hyperbolic tangent functions to introduce non-linearity, this empowers SVM to handle a wide range of data complexities and enable effective classification. In this experiment, the optimal parameters established in previous trials were maintained while altering the kernel function. Notably, it is evident that the linear kernel outperforms the others in accuracy. Table 6 illustrates the impact of different kernel choices on the results.

Based on the outcomes of these experiments, it can be deduced that the most effective parameters for fault diagnosis in PV modules are a C value of 10, a gamma value set to 'scale,' and the utilization of a linear kernel. Supplementary Fig. 8, illustrates the confusion matrix generated from the SVM classification. In the context of a non-uniform dataset, a confusion matrix provides a detailed breakdown of a classification models performance by revealing the distribution of true positive, false positive, true negative, and false negative predictions for each class. This is especially crucial when dealing with imbalanced datasets. The matrix allows for a nuanced evaluation of how well the model is distinguishing between different classes, enabling insights into potential biases or weaknesses. The visual representation of image transformations at each autoencoder layer is pivotal for a nuanced analysis of the models internal mechanisms in fault detection. Supplementary Fig. 9, provides a visual narrative of how the autoencoder processes input images across various layers, unravelling the hierarchical extraction of features. By observing these transformations, specific visual cues and patterns that the model deems significant in identifying faults can be identified.

This visual insight, complemented by quantitative metrics such as Root Mean Squared Error (RMSE), Mean Absolute Error (MAE), R squared and Correlation Coefficient, not only enhances the transparency of the autoencoders decision-making but also offers a quantitative assessment of the reconstruction accuracy. The R squared, RMSE, MAE and Correlation coefficient values are 1.0000, 0.1160, 0.0420 and 0.9977 respectively. The amalgamation of visual and quantitative analyses facilitates a more comprehensive understanding of the autoencoders performance. Additionally, the inclusion of Supplementary Fig. 10, representing the t-SNE graph, adds another layer of analysis. The t-SNE graph provides a visualization of the data in a reduced-dimensional space, helping to identify patterns and clusters. The observation of misclassifications in the t-SNE graph highlights areas where the autoencoder may encounter challenges in fault detection. To

Table 5
Effect of gamma in the classification accuracy.

gamma	scale	auto
Accuracy (%)	97.30	97.30
Precision (%)	97.32	97.32
Recall (%)	97.30	97.30
F1 (%)	97.29	97.29
Training time (s)	3.42	4.71
Prediction time (s)	1.47	1.59

Table 4
Effect of C value in the classification accuracy.

C	0.01	0.1	1	10	100	200
Accuracy (%)	37.14	83.02	94.92	97.30	97.14	97.14
Precision (%)	35.30	84.50	95.01	97.32	97.14	97.14
Recall (%)	37.14	83.02	94.92	97.30	97.14	97.14
F1 (%)	30.86	83.28	94.88	97.29	97.13	97.13
Training time (s)	18.71	10.72	4.08	3.42	4.27	4.01
Prediction time (s)	5.79	4.91	2.04	1.47	1.56	1.69

Table 6
Effect of kernel in the classification accuracy.

kernel	linear	poly	rbf	sigmoid
Accuracy (%)	98.57	97.46	97.30	73.81
Precision (%)	98.57	97.48	97.32	77.58
Recall (%)	98.57	97.46	97.30	73.81
F1 (%)	98.57	97.45	97.29	74.14
Training time (s)	2.07	3.35	3.42	2.67
Prediction time (s)	0.44	0.70	1.47	0.71

address these challenges, the decision was made to increase the number of features and then to perform classification.

The models outstanding performance with an accuracy, precision, recall, and F1 score of 98.57% holds significant promise for practical applications. The precision and recall values imply that the model is adept at identifying and correctly classifying instances of faults in PV modules, crucial for ensuring the reliability and efficiency of solar energy systems. The quick training time of 2.07 s and rapid prediction time of 0.44 s suggest that the model can deliver accurate diagnoses swiftly, making it well-suited for real-time fault detection scenarios. Overall, these results showcase the models potential as a valuable tool in enhancing the maintenance and performance monitoring of photovoltaic systems.

Comparison with other cutting-edge-works

In this section, a comparative analysis is conducted to showcase the superior performance of the proposed method when compared to state-of-the-art approaches documented in the existing literature. Table 7 provides a comparison of the effectiveness of various techniques against the recommended methodology. The results presented in Table 7 clearly indicate that the proposed approach outperforms all previous studies, achieving an impressive classification accuracy of 98.57%.

Conclusion

This research presents a comprehensive methodology for the identification and diagnosis of faults in PV modules, utilizing RGB photos captured by UAVs. By extending the scope of fault detection to encompass both electrical and aesthetic anomalies, implementing data augmentation techniques to enrich dataset diversity, employing autoencoders for effective feature extraction, and fine-tuning classification using SVM, the study yielded an impressive accuracy rate of 98.57%, even when working with a non-uniform dataset. The precision, recall, and F1 score also reached notable values, each at 98.57%. The efficiency of the model is reflected not only in its accuracy but also in the computational aspects. The training time required for the system was minimal, clocking in at 2.07 s, while the prediction time was also notably swift at 0.44 s. These findings offer promising implications for the solar energy industry, providing a robust framework to enhance the maintenance and operational efficiency of PV installations. The groundbreaking advancements achieved in the solar energy industry hold tremendous promise for enhancing the reliability and efficiency of PV installations, playing a crucial role in the global transition to sustainable energy sources. This research contributes significantly to improving maintenance practices and operational efficiency within the solar sector, thereby fostering the overall stability and growth of renewable energy. However, inherent limitations, such as concerns about dataset representativeness, sensitivity to technological changes and dependency on image quality necessitate a strategic roadmap for future work. Addressing these challenges involves expanding and diversifying datasets, integrating multi-sensor data, implementing continuous model updating, exploring adaptive image processing techniques, and enhancing the models decisions. Furthermore, the development of human-in-the-loop systems emerge as essential components for ensuring a resilient fault detection mechanism adaptable to evolving real-world conditions. In essence, this research not only signifies a significant leap in solar technology but underscores the importance of addressing challenges to propel us towards a sustainable and resilient energy future.

Funding

No funding was associated with this study.

Table 7
Comparison with other state-of-art techniques.

Fault diagnosis approach	Classification Accuracy (%)	References
CNN	94.41	[26]
Pre-trained VGG16	95.40	[27]
CNN	79.06	[28]
Deep Solar Eye	97.80	[29]
CNN	97.90	[30]
Yolo V3	96.30	[31]
Autoencoders & SVM	98.57	Proposed

CRediT authorship contribution statement

C.V. Prasshanth: . S. Naveen Venkatesh: . V. Sugumaran: . Mohammadreza Aghaei: Writing – review & editing, Validation, Supervision, Resources, Methodology, Funding acquisition, Data curation, Conceptualization.

Declaration of competing interest

The authors declare that they have no known competing financial interests or personal relationships that could have appeared to influence the work reported in this paper.

Data availability

No data was used for the research described in the article.

Appendix A. Supplementary data

Supplementary data to this article can be found online at https://doi.org/10.1016/j.seta.2024.103674.

References

[1] Tiwari GN, Mishra RK, Solanki SC. Photovoltaic modules and their applications: a review on thermal modelling. Appl Energy 2011;88. https://doi.org/10.1016/j.apenergy.2011.01.005.
[2] Vieira RG, de Araújo FMU, Dhimish M, Guerra MIS. A comprehensive review on bypass diode application on photovoltaic modules. Energies (Basel) 2020;13. https://doi.org/10.3390/en13102472.
[3] Qin J, Hu E, Li X. Solar aided power generation: a review. Energy Built Environ 2020;1. https://doi.org/10.1016/j.enbenv.2019.09.003.
[4] Pillai DS, Rajasekar N. A comprehensive review on protection challenges and fault diagnosis in PV systems. Renew Sustain Energy Rev 2018;91. https://doi.org/10.1016/j.rser.2018.03.082.
[5] Madeti SR, Singh SN. Modeling of PV system based on experimental data for fault detection using kNN method. Sol Energy 2018;173. https://doi.org/10.1016/j.solener.2018.07.038.
[6] Viswanathan PC, Venkatesh SN, Dhanasekaran S, Mahanta TK, Sugumaran V, Lakshmaiya N, et al. Deep learning for enhanced fault diagnosis of monoblock centrifugal pumps: spectrogram-based analysis. Machines 2023;11:874. https://doi.org/10.3390/MACHINES11090874.
[7] Kellil N, Aissat A, Mellit A. Fault diagnosis of photovoltaic modules using deep neural networks and infrared images under algerian climatic conditions. Energy 2023;263. https://doi.org/10.1016/j.energy.2022.125902.
[8] Jerome Vasanth J, Naveen Venkatesh S, Sugumaran V, Mahamuni VS. Enhancing photovoltaic module fault diagnosis with unmanned aerial vehicles and deep learning-based image analysis. International Journal of Photoenergy 2023;2023. https://doi.org/10.1155/2023/8665729.
[9] Sridharan NV, Sugumaran V. Visual fault detection in photovoltaic modules using decision tree algorithms with deep learning features. Energy Sources Part A 2021. https://doi.org/10.1080/15567036.2021.2020379.
[10] Tsanakas JA, Chrysostomou D, Botsaris PN, Gasteratos A. Fault diagnosis of photovoltaic modules through image processing and canny edge detection on field thermographic measurements. Int J Sustain Energ 2015;34. https://doi.org/10.1080/14786451.2013.826223.
[11] Hu Y, Gao B, Song X, Tian GY, Li K, He X. Photovoltaic fault detection using a parameter based model. Sol Energy 2013;96. https://doi.org/10.1016/j.solener.2013.07.004.
[12] Jaffery ZA, Dubey AK, Irshad HA. Scheme for predictive fault diagnosis in photovoltaic modules using thermal imaging. Infrared Phys Technol 2017;83:182–7. https://doi.org/10.1016/J.INFRARED.2017.04.015.
[13] Mehedi IM, Salam Z, Ramli MZ, Chin VJ, Bassi H, Rawa MJH, et al. Critical evaluation and review of partial shading mitigation methods for grid-connected PV

system using hardware solutions: the module-level and array-level approaches. Renew Sustain Energy Rev 2021;146:111138. https://doi.org/10.1016/J.RSER.2021.111138.
[14] W.H. Lopez Pinaya S. Vieira R. Garcia-Dias A. Mechelli Autoencoders Machine Learning: Methods and Applications to Brain Disorders 2020 193 208 10.1016/B978-0-12-815739-8.00011-0.
[15] Jia F, Lei Y, Guo L, Lin J, Xing S. A neural network constructed by deep learning technique and its application to intelligent fault diagnosis of machines. Neurocomputing 2018;272. https://doi.org/10.1016/j.neucom.2017.07.032.
[16] Köntges M, Kurtz S, Packard CE, Jahn U, Berger K, Kato K, et al. Review of failures of photovoltaic modules. IEA-PVPS 2014;T13–01:2014.
[17] Dolara A, Lazaroiu GC, Leva S, Manzolini G, Votta L. Snail trails and cell microcrack impact on PV module maximum power and energy production. IEEE J Photovolt 2016;6. https://doi.org/10.1109/JPHOTOV.2016.2576682.
[18] Han H, Dong X, Li B, Yan H, Verlinden PJ, Liu J, et al. Degradation analysis of crystalline silicon photovoltaic modules exposed over 30 years in hot-humid climate in China. Solar Energy 2018:170. https://doi.org/10.1016/j.solener.2018.05.027.
[19] Sánchez-Friera P, Piliougine M, Peláez J, Carretero J, De Cardona MS. Analysis of degradation mechanisms of crystalline silicon PV modules after 12 years of operation in Southern Europe. Progress in Photovoltaics: Research and Applications 2011;19. https://doi.org/10.1002/pip.1083.
[20] Chandel SS, Nagaraju Naik M, Sharma V, Chandel R. Degradation analysis of 28 year field exposed mono-c-si photovoltaic modules of a direct coupled solar water pumping system in western himalayan region of India. Renew Energy 2015;78:193–202. https://doi.org/10.1016/J.RENENE.2015.01.015.
[21] Mumuni A, Mumuni F. Data augmentation: a comprehensive survey of modern approaches. Array 2022;16. https://doi.org/10.1016/j.array.2022.100258.
[22] Rubio L-, Palomo E, Domínguez E, Chen S, Guo W. Auto-encoders in deep learning—a review with new perspectives. Mathematics 2023;11:1777. https://doi.org/10.3390/MATH11081777.
[23] Zhai J, Zhang S, Chen J, He Q. In: Autoencoder and Its Various Variants; 2019. https://doi.org/10.1109/SMC.2018.00080.
[24] Awad M, Khanna R. Support vector machines for classification. Efficient Learning Mach 2015:39–66. https://doi.org/10.1007/978-1-4302-5990-9_3.
[25] Evgeniou T, Pontil M. support vector machines: theory and applications. lecture notes in computer science (including subseries lecture notes in artificial intelligence and lecture notes in Bioinformatics) 2001;2049 LNAI:249–57. https://doi.org/10.1007/3-540-44673-7_12.
[26] Sridharan NV, Sugumaran V. Convolutional neural network based automatic detection of visible faults in a photovoltaic module. Energy Sources Part A 2021. https://doi.org/10.1080/15567036.2021.1905753.
[27] S. Naveen Venkatesh V. Sugumaran Fault detection in aerial images of photovoltaic modules based on deep learning. IOP Conf Ser Mater Sci Eng. 2021; 1012. https://doi.org/10.1088/1757-899x/1012/1/012030.
[28] Li X, Yang Q, Wang J, Chen Z, Yan W. Intelligent fault pattern recognition of aerial photovoltaic module images based on deep learning technique. 2018.
[29] Mehta S, Azad AP, Chemmengath SA, Raykar V, Kalyanaraman S. In: Deepsolareye: power loss prediction and weakly supervised soiling localization via fully convolutional networks for solar panels; 2018. https://doi.org/10.1109/WACV.2018.00043.
[30] Li X, Yang Q, Lou Z, Yan W. Deep learning based module defect analysis for large-scale photovoltaic farms. IEEE Trans Energy Convers 2019;34. https://doi.org/10.1109/TEC.2018.2873358.
[31] Wang J, Zhao B, Yao X. In: PV abnormal shading detection based on convolutional neural network; 2020.. https://doi.org/10.1109/CCDC49329.2020.9164630.